# Surface enhanced SHG from macrocycle, catenane and rotaxane thin films: experiments and theory.

Imad Arfaoui[a], Veronika Bermudez[b], Celine De Nadai[c], Jukka-Pekka Jalkanen[e], François Kajzar[b], David Leigh[d] , Monika Lubomska[a], Sandra M. Mendoza[a], Jacek Niziol[b], Petra Rudolf[a], and Francesco Zerbetto[e]

[a]Materials Science Centre, University of Groningen, Nijenborgh 4, NL-9747 AG Groningen The Netherlands
[b]Commissariat à l'Energie Atomique, DRT – LITEN, DSEN/GENEC/L2C, CEA/Saclay,F-91191 Gif sur Yvette, France
[c]Laboratoire Interdisciplinaire de Spectroscopie Electronique, Facultés Universitaires Notre-Dame de la Paix, 61 rue de Bruxelles, B-5000 Namur, Belgium
[d]School of Chemistry, University of Edinburgh, The King's Buildings, West Mains Road, Edinburgh EH9 3JJ, United Kingdom
[e] Dipartimento di Chimica "G. Ciamician", Università di Bologna, via F. Selmi 2 I-40126 Bologna, Italy

## ABSTRACT

Surface enhanced second harmonic generation experiments on supramolecules: macrocycles, catenanes and rotaxanes, monolayers and multilayers deposited by vacuum evaporation on silver layers are reported and described. The measurements show that the molecules are ordered in thin films. The highest order is observed in the case of macrocycles and the lowest in thin films of fumaramide [2] rotaxanes. Also a better ordering is observed in the case of monolayers. The observed second harmonic generation activity is interpreted in terms of electric field induced second harmonic generation. The electric field contributing to SHG signal is created by silver atoms on the surface of silver layers. The measured second order NLO susceptibilities for a fumaramide [2] rotaxane is compared with that obtained by considering only EFISH contribution to SHG intensities. The electric filed on the surface of silver layer is calculated using TINKER molecular mechanics/dynamics software and the Embedded Atom model. An excellent agreement is observed between the calculated and the measured SHG susceptibilities.

**Keywords**: catenanes, rotaxanes, molecular motors, second harmonic generation, surface effects, X-Ray photoelectron spectroscopy

## 1. INTRODUCTION

Catenanes and rotaxanes are new classes of molecules composed from moving parts. They represent a great interest for potential applications in photonics, particularly in all optical and electro - optical switching. The catenanes are fundamentally made from interlocked macrocycles with ability of a relative movement of one macrocycle with respect to another one(s). In the case of rotaxanes, the macrocycle can move (shuttling) and/or circumrotate around a thread. The shuttling movement of the macrocycle is limited by stoppers located at both ends of the thread (e.g. two phenyl rings in the case of fumaramide [2] rotaxane). A clipping movement in rotaxanes is also possible provided that the thread is sufficiently long and flexible and the movement can be excited by e.g. light via conformational changes of thread due a photoizomerization process.

Large catenanes ($Mw=10^5$) are present in nature in DNA as intermediates during the replication, transcription, and recombination process. Since the first two-ring catenane was obtained in early sixties, smaller synthetic catenanes (Mw=103) have attracted the interest of chemists and physicists. Both catenanes and rotaxanes can be functionalized and

Organic Photonic Materials and Devices VII, edited by James G. Grote, Toshikuni Kaino, François Kajzar, Proceedings of SPIE Vol. 5724 (SPIE, Bellingham, WA, 2005)
0277-786X/05/$15 · doi: 10.1117/12.592379

their physico-chemical properties can be tailored by an adequate substitution. They can be also processed into good optical quality thin films by vacuum evaporation. The linear and nonlinear optical properties of these films were studied by various techniques and the results of these investigations are presented and discussed. An emphasis is put on Surface Enhanced Second Harmonic Generation (SE SHG) experiments, which combined with theoretical calculations lead to molecular characteristics determination.

## 2. EXPERIMENTAL DETAILS

The synthesis of the benzylic amide [2]catenane (1,7,14,20-tetraaza-2,6,15,19-tetraoxo-3,5,9,12,16,18,22,25-tetrabenzocyclohexacosane)-(1',7',14',20'-tetraaza-2',6',15',19'-tetraoxo-3',5',9',12',16',18',22',25'-tetrabenzocyclohexaco - sane), the fumaramide [2]rotaxane ([2]-(1,7,14,20-tetraaza-2,6,15,19-tetraoxo-3,5,9,12,16,18,22,25-tetrabenzo - cyclohexacosane)-(E)-(N,N'-bis(2',2'-diphenylethyl)-2'-butendiamide)) and the benzylic amide macrocycle (1,7,14,20-tetraaza-2,6,15,19-tetraoxo-3,5,9,12,16,18,22,25-tetrabenzocyclohexosane) which were studied in this work is described elsewhere[1,2,3,4,5]. For simplicity, we will refer to them in the text as *catenane*, *fumaramide [2]rotaxane* and *macrocycle*, respectively. Fig. 1 shows the chemical structure of the three compounds.

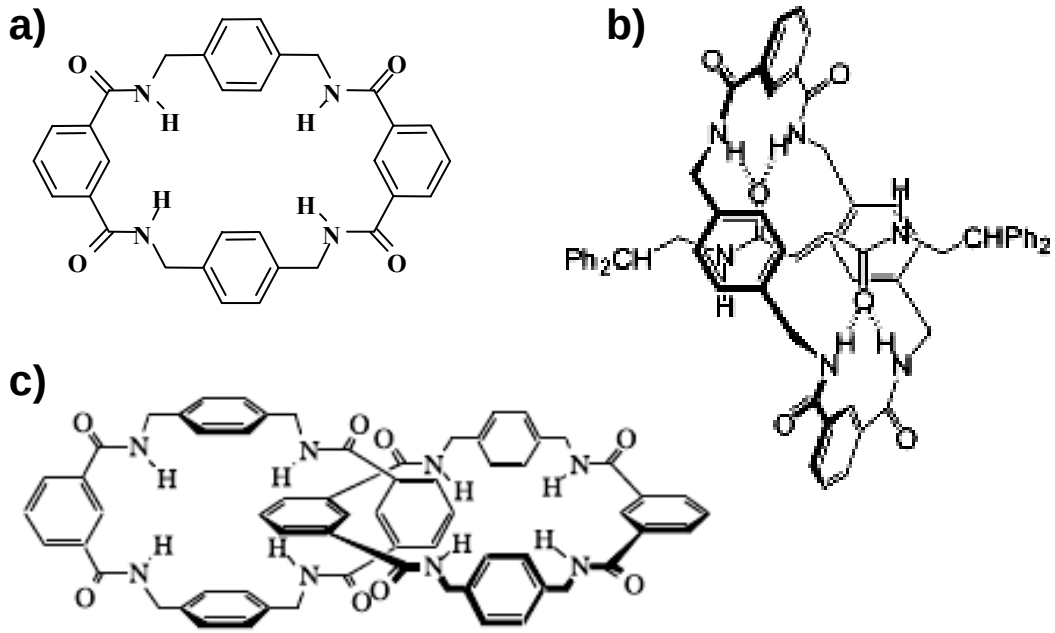


Figure 1. a) Chemical structure of (a) benzylic amide macrocycle; (b) fumaramide [2]rotaxane, composed buy a macrocycle locked onto a thread; and (c) benzylic amide [2]catenane, composed by two interlocked macrocycles.

For the study of ordering by surface enhanced second harmonic generation technique (SE SHG), thin films of macrocyle, catenane and rotaxane were prepared by ultra high vacuum (UHV) evaporation onto $SiO_2$ substrates for measurements in transmission on polycrystalline Ag substrates for measurements in reflection. Ag substrates were obtained by vacuum evaporation onto freshly cleaved mica. The silver layer thickness was 400 nm (non-transparent). Prior to molecules deposition, the Ag films were cleaned *in situ* by cycles of argon ion bombardment until no contaminants could be detected in the spectra measured by high resolution electron energy loss spectroscopy (HREELS) or X-ray Photoelectron Spectroscopy (XPS). These techniques are capable of detecting a few hundredth of a monolayer of contaminants.

The organic molecules were sublimed in a UHV system (base pressure of $2x10^{-10}$ Torr) onto the substrates kept at 300 K using a custom built cell which consisted of a Pyrex crucible topped with a 2 mm stainless steel collimator. The crucible was heated resistively to 500 K for the macrocycle and 470 K for the catenane and fumaramide [2]rotaxane with the temperature being measured by a chromel-alumel junction fixed at the tube exit. Exposures were monitored using an uncalibrated Bayard-Alpert ionization gauge. The film thickness was found 137 Å for catenane film, 1073 Å for macrocycle film as measured with a profilometer and 100 Å for fumaramide [2]rotaxane film film measured by atomic force microscopy.. The molecular thin films have been characterized by high resolution electron energy loss spectroscopy (HREELS) or X-ray photoemission spectroscopy (XPS) *in situ* in the UHV system in order to check the cleanliness and the coverage of the molecules. In order to prepare a monolayer film of either macrocyle, catenane and fumaramide [2]rotaxane, we first deposited a thicker film and then annealed it *in situ* to induce desorption of all molecules not chemisorbed to Ag. In the case of macrocycle and catenane the characteristic monolayer spectrum was identified by HREELS after this treatment[6,7,8]. With this reference, spectra corresponding to less than or more than a monolayer can be identified with confidence. The film thickness was estimated to be one monolayer for both catenane and macrocycle films. In a similar way we determined by XPS that fumaramide [2]rotaxane sublimes intact and the monolayer coverage could be reached.

The experimental set–up used for SE SHG measurements is shown schematically in Fig. 2. The measurements were performed using a Q switched Nd:YAG laser, operating at 1064 nm fundamental wavelength with 10 pps operation rate and 13 ns pulse duration. A transmission geometry was used in some cases. However, most experiments were performed in reflection, as shown in Fig. 2. The sample and a dichroic mirror, reflecting the harmonic 532 nm wavelength, were mounted on rotation stages. Both rotations were synchronized. The direction of the polarization of incident wave was varied continuously by rotating a half-wave plate at fundamental wavelength. The harmonic beam polarization was checked with a Glan-Thomson polarizer at a fixed direction during the experiments.

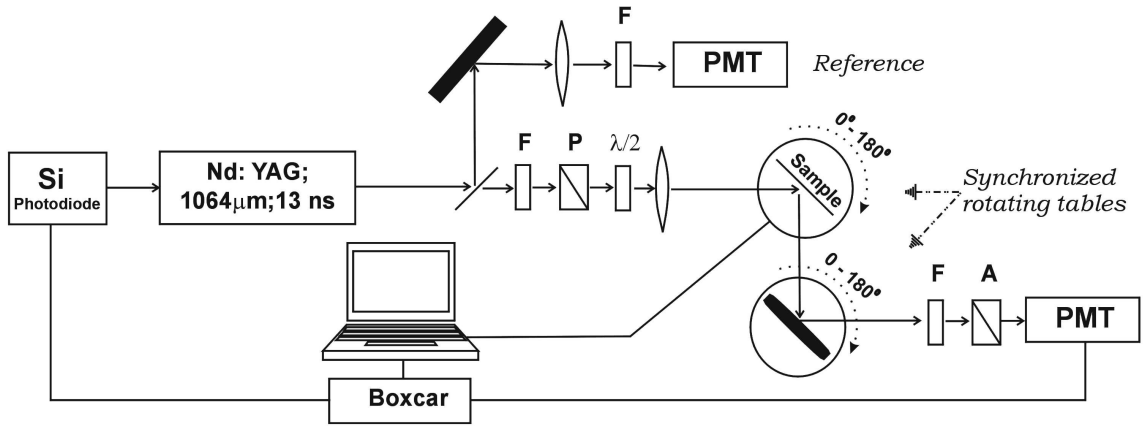


Figure 2. Schematic representation of experimental set-up used for SE SHG experiments. Details are given in text.

## 3. RESULTS AND DISCUSSIONS

### 3.1. SURFACE ENHANCED SECOND HARMONIC GENERATION EXPERIMENTS

Figure 3 shows harmonic fields detected from a fumaramide [2]rotaxane monolayer and from pure silver surface. A small signal from silver layers is observed, which is significantly weaker than that coming from the monolayer. For the fumaramide [2]rotaxane monolayer we observe a strong dependence of SHG intensity on fundamental beam polarization direction. The angles 0 and 180 degrees correspond to p–type polarization of this beam. The harmonic polarization is fixed to be p-type. This behaviour is characteristic for poled thin films, characterized by two non zero $\chi^{(2)}$ $(-2\omega;\omega,\omega)$ tensor components: $\chi^{(2)}_{sp}$ and $\chi^{(2)}_{pp}$. It corresponds to the thin film symmetry ∞mm, with rotation axis perpendicular to the

thin film substrate. Both susceptibilities are expressed by configurational averages, assuming (for the sake of simplicity) that there is only one non zero first hyperpolarizability β component, $\beta_{zzz}$:

$$\chi_{pp}^{(2)}(-2\omega;\omega,\omega) = NF\beta_{zzz}(-2\omega;\omega,\omega) < \cos^3\Theta > \quad (1)$$

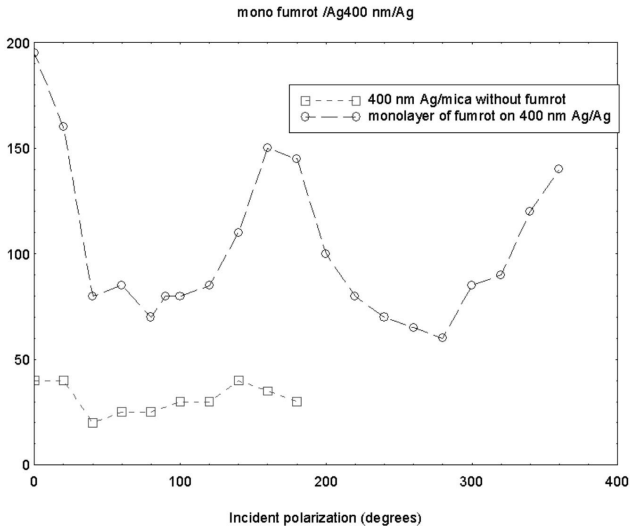


Figure 3. Fundamental beam polarization dependence of SHG intensity from a monolayer of fumaramide [2]rotaxane (open circles) and from a silver layer (squares). The harmonic beam polarization is of p type.

and

$$\chi_{sp}^{(2)}(-2\omega;\omega,\omega) = \frac{1}{2}NF\beta_{zzz}(-2\omega;\omega,\omega) < \sin^2\Theta\cos\ \Theta > \quad (2)$$

where N is the density of molecules, F is the local field factor and Θ is the angle between the symmetry axis and the probing optical field direction. Thus, the ratio of the two nonzero $\chi^{(2)}$ tensor components

$$a = \frac{\chi_{pp}^{(2)}(-2\omega;\omega,\omega)}{\chi_{sp}^{(2)}(-2\omega;\omega,\omega)} \quad (3)$$

is a measure of the order. It take the values between 1 and ∞ . In Figs. 4 - 6 are displayed, in polar coordinates, dependences of the second order non linear optical susceptibility $\chi^{(2)}$ on the angle between the fundamental and harmonic field polarizations for the studied mono – and multilayers of a macrocycle, catenane and fumaramide [2]rotaxane, respectively. As already mentioned, the harmonic beam polarization is selected to be of p type. All susceptibilities are normalized, independently, to the maximum value. The sphere corresponds to $a = 1$ and the line to $a = \infty$. The width of the distribution is thus a fingerprint of the molecular order. The *a* parameters, determined for the studied thin films, are listed in Table 1. From figures 4 - 6 and from the data in this table it is clearly seen that larger order is observed for monolayers than for multilayers, as expected. Among the studied compounds the highest order is see in thin films of macrocycle. Due to their planar structure they orient preferentially parallel to the substrate during the vacuum deposition,

as expected. Similar behaviour, with slightly less order, is also observed in catenanes. This kind of orientation was also observed in optical birefringence measurements on vacuum deposited thin films of these supramolecules[17]. Less order in fumaramide [2]rotaxane thin films can be also well understood as due to the chemical structure of these molecules.

To explain the origin of the large SHG signal we made theoretical calculations for the field experienced by the molecules on a silver surface. It is well known that the silver surface breaks isotropy in presumably isotropic thin films deposited on it because of large electric field created by silver atoms on the surface. For the sake of comparison the calculations were performed for silver and gold surfaces.

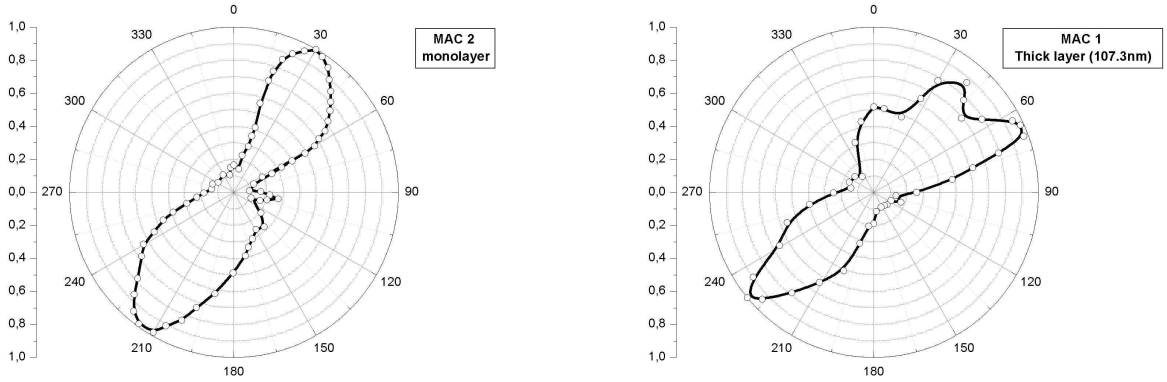


(a) (b)

Figure 4. Polarization dependence (in polar coordinates) of $\chi^{(2)}$ susceptibility for a monolayer (a) and for a multilayer (b) of macrocycle.

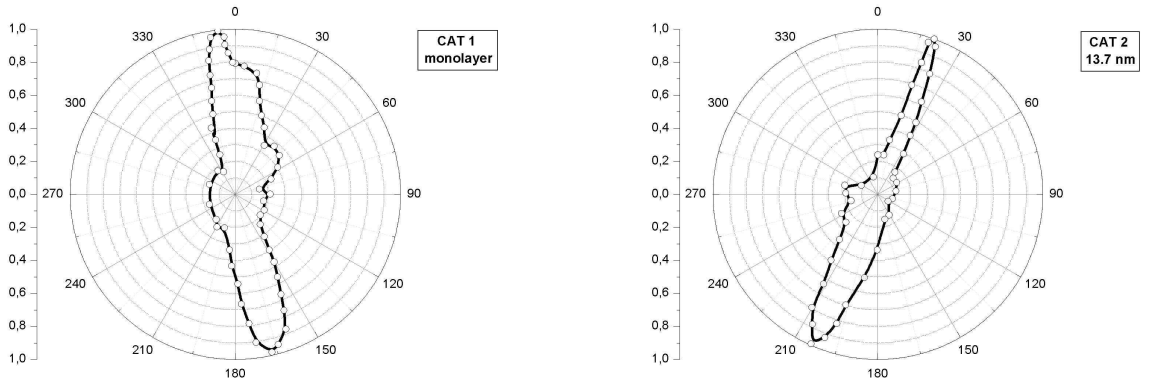


(a) (b)

Figure 5. Polarization dependence (in polar coordinates) of $\chi^{(2)}$ susceptibility for a monolayer (a) and for a 13.7 nm thick multilayer of catenane (b).

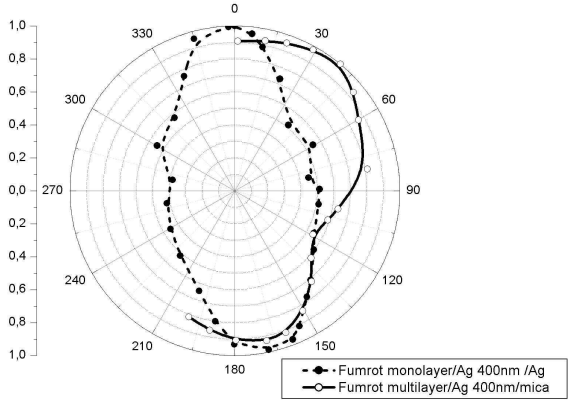


Figure 6. Polarization dependence (in polar coordinates) of $\chi^{(2)}$ susceptibility for a monolayer (dashed line) and for a multilayer (continous line) of fumaramide [2]rotaxane.

Table 1.

Values of a parameter (a = $\chi^{(2)}_{pp}(-2\omega;\omega,\omega) / \chi^{(2)}_{sp}(-2\omega;\omega,\omega)$ ) for the studied supramolecules.

| Thin film | Structure | a |
|---|---|---|
| macrocycle | Multilayer | 6.6 |
| " | Monolayer | 7.2 |
| catenane | Multilayer | 5.5 |
| " | Monolayer | 4.8 |
| fumaramide [2]rotaxane | Multilayer | 1.3 |
| " | Monolayer | 3.0 |

### 3.2 MOLECULAR MECHANICS STUDIES

The calculations were performed for a single molecule of fumaramide [2]rotaxane deposited on Au(111) and Ag(111) surfaces. Its structure was minimized using TINKER molecular mechanics/dynamics software package[9,10,11,12] The Embedded Atom Model[10] was used in describing the metal-metal interactions, MM3 force field[10] for organic-organic part and a modified Morse potential (Eq. (4)) in description of metal-organic interactions.

$$U(r_{ij}) = -\varepsilon * \left(1 - \left\{1 - \exp\left[-A(r_{ij} - r_{ij}^{*})\right]\right\}^{2}\right) \qquad (4)$$

In addition, the charge equilibration scheme of Rappe et al.[10,] was applied throughout the whole system. This method can be used to study the evolution of partial charges when chemical environment or molecular geometry changes. The metal-organic interaction model was calibrated to produce experimental desorption geometries and energies of small organic fragments consisting of similar chemical groups that can be found in fumaramide[2]rotaxane. A metal(111) surface model consisting of five layers of 20 by 20 atoms was used and the lowest layer of metal atoms was kept fixed during the calculations. The top four layers of the surface model were allowed to relax or reconstruct to achieve lowest energy.

The charge distribution generated by the adsorption of the fumaramide [2]rotaxane molecule on the metal(111) surface was investigated further with Delphi4 program[13] to compute the electrostatic potential and the electric field on top of the surface. In Fig.7, an example of charge distribution on Ag(111) surface is illustrated (left). The figure on the right shows the orientation of the fumaramide [2]rotaxane on the surface. According to the calculations, the fumaramide [2]rotaxane molecule orients itself on a surface in a way that two carbonyl groups and one of the benzene rings of both

the macrocycle and the thread are close to the surface, changing the metal charge distribution. As can be seen from the figure, the surface silver atoms undergo slight changes in partial charges, which are largest on atoms closest to carbonyl groups. In the beginning of the calculation, the surface is charge neutral, but as the fumaramide [2]rotaxane is adsorbed some atoms become positively charged while others obtain a small negative charge. The second group of metal atoms showing positive charges are the ones lying directly under one of the benzene rings of the thread.

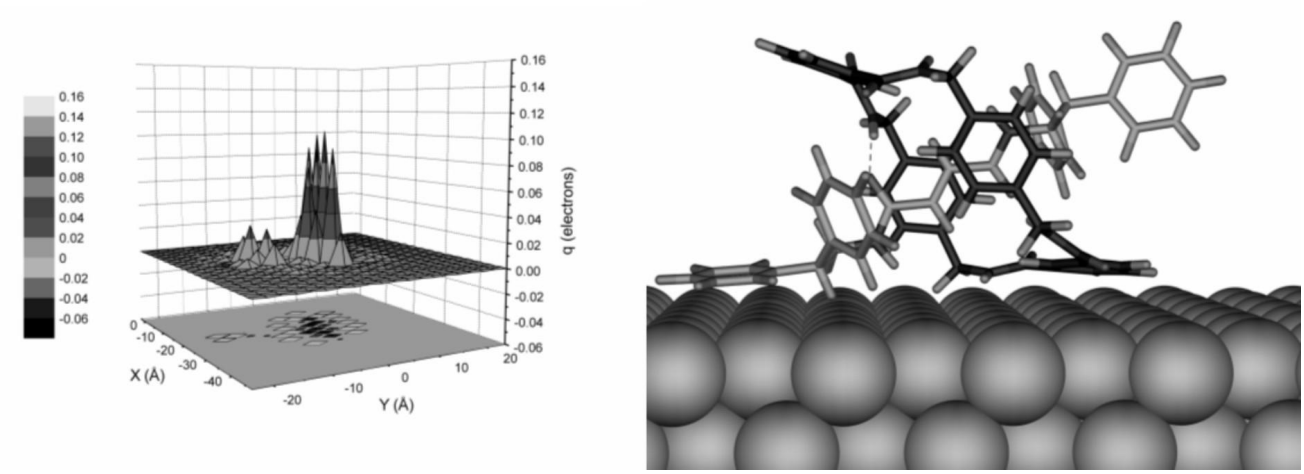


Figure 7. The partial charges on top layer of silver atoms of Ag(111) surface (left). The orientation of the fumaramide [2]rotaxane molecule on Ag(111) surface (right). The carbon atoms belonging to the thread are colored green, while the ones belonging to the macrocycle are black.

The electrostatic potential and the electric field were studied using Poisson-Boltzmann algorithms in Delphi4 program[13,14]. For this purpose, only the top layer metal atoms that had $|q|>0.001$ electrons were considered. The charges generated on top layer metal atoms by the fumaramide [2]rotaxane adsorption were used but the rotaxane molecule itself was excluded from the field calculations to illustrate the electric field experienced by the organic when it is adsorbed to the surface. The electric field was calculated on top of the metal surface on ~17 000 evenly distributed points which were selected so, that they would be inside the space occupied by the rotaxane van der Waals volume. An example of the resulting electric fields is illustrated in Fig 9. As it can be seen from this figure, the electric field is inhomogeneous and two clearly positive areas can be distinguished. The largest positive field occurs just below the rotaxane carbonyl groups. The second, weaker field occurs below the thread benzene ring. The calculated average field strength inside the rotaxane volume of space is roughly 15 MV/cm and disappears ~9 Å away from the surface. This short depth of the electric field is confirmed by experiment. Indeed, as it is seen from Fig. 8 we observe almost the same SHG intensity from a monolayer than from multilayer. Thus no dependence of the thin film thickness.

Calculations were repeated for fumaramide[2]rotaxane/Au(111) system and the obtained field strength was lower, about 7 MV/cm. The metal atoms on top layer of the Au(111) surface show larger variety on metal partial charges, but the field is weakened by the presence of negatively charged atoms, whereas with Ag(111) the atoms are, on average, more positively charged.

### 3.2 COMPARISON WITH EXPERIMENT

Using the theoretical values of electric field on silver layer we have calculated the $\chi^{(2)}$ $(-2\omega;\omega,\omega)$ susceptibility assuming that the SHG activity is nothing else than electric field induced second harmonic generation (EFISH). Indeed, in past, we observed only small, under pm/V $\chi^{(2)}$ $(-2\omega;\omega,\omega)$ susceptibilities for evaporated pristine films of catenanes and fumaramide [2]rotaxane [15,18]. The comparison was done for fumaramide [2]rotaxane thin films, for which the calculations were performed. Due to relatively complex experimental geometry the SHG intensities from fumaramide [2]rotaxane thin films were calibrated by SHG on poled polymethyl methacrylate (PMMA) thin films functionalized with disperse red #1

molecule (65:35 w%). The poled films of this composite material were independently calibrated with SHG from an α-quartz single crystal. The values used for α-quartz for calibration is that reported in literature by Choy and Byer[16] ($d_{11}'(-2\omega;\omega,\omega) = \chi^{(2)}_{11}(-2\omega;\omega,\omega)/2 = 0.5$ pm/V). Consequently, assuming that only the monolayer with thickness of 9 Å contributes to SHG signal we obtain for $\chi^{(2)}(-2\omega;\omega,\omega)$ for the studied fumaramide [2]rotaxane a value of 23.4 pm/V.

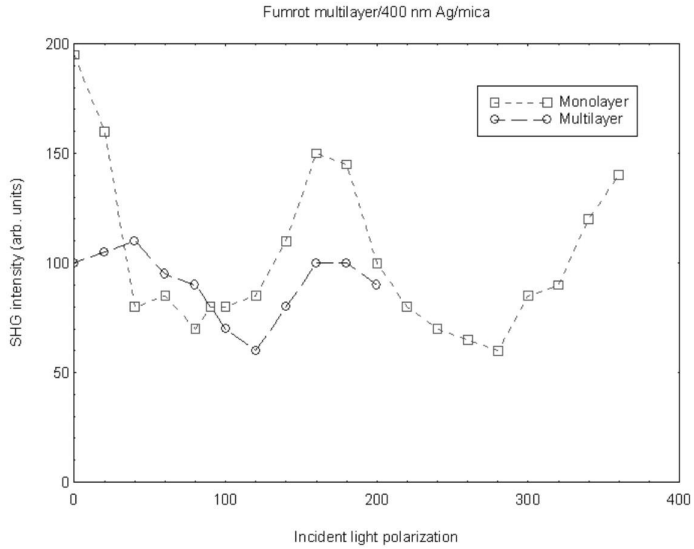


Figure 8. SHG intensity from a multilayer and a monolayer in function of the angle (in degrees) between the fundamental beam and the harmonic (fixed to be p type) polarization directions.

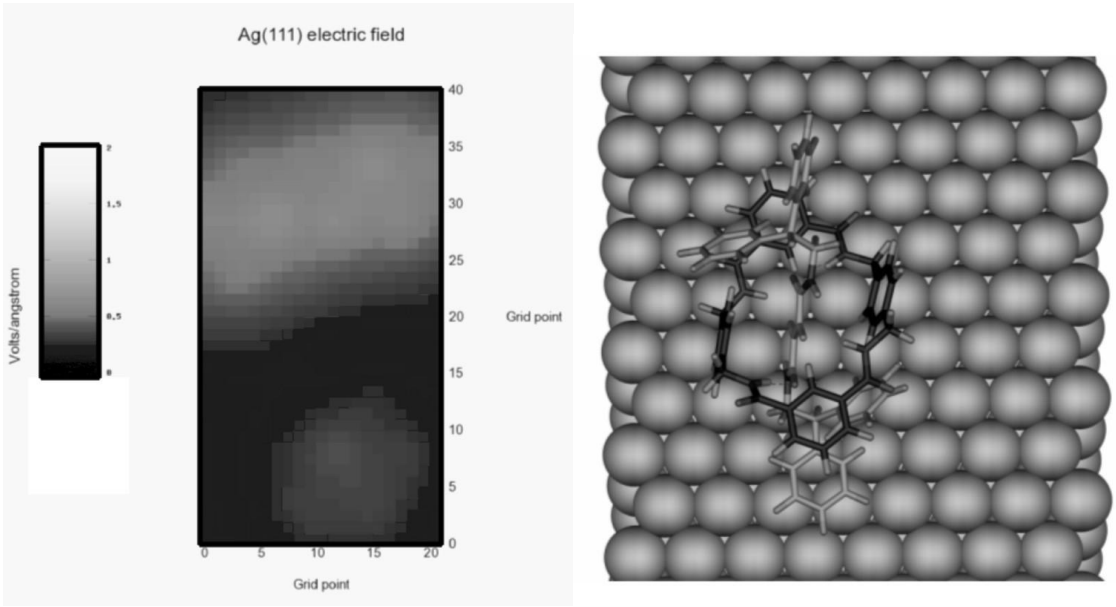


Fig. 9. The electric field on top of the Ag(111) surface(left). The distance to surface is 1.62 Å, which corresponds to shortest surface normal of any rotaxane atom. The fumaramide [2]rotaxane orientation on the Ag(111) surface is shown on the figure right.

The theoretical value derived from the electric field calculations is obtained as follows. For EFISH experiments the SHG susceptibility can be expressed as follows:

$$\chi^{(2)}(-2\omega;\omega,\omega) = NF\gamma(-2\omega;\omega,\omega,0)E \tag{5}$$

where, similarly as before N and F are, respectively, the molecule density and local field factor, $\gamma(-2\omega;\omega,\omega,0)$ is EFISH molecular second hyperpolarizability and E is the applied electric field(in this case the calculated one). Assuming $\gamma(-2\omega;\omega,\omega,0) \approx \gamma(-3\omega;\omega,\omega,\omega)$ and taking the THG values determined previously for thin films of fumaramide [2]rotaxane under consideration ($\gamma(-3\omega;\omega,\omega,\omega) = 1.49\text{x}10^{-34}$ esu ) as well as the calculated electric field on Ag surface E=15 MV/cm one obtains $\chi^{(2)}_{EFISH}$ = 24.2 pm/V. It is in surprisingly good agreement with the measured value, taking account of all simplifications and approximations made.

## 4. CONCLUSIONS

The present study shows that catenanes and rotaxanes represent a new class of potentially interesting molecules, with mobile parts, for application in photonics. Similarly as polymers these molecules can be functionalized and their optical and physico-chemical properties can be modified. Both molecules can be processed into thin film with a good optical quality. The films are characterized by optical birefringence which is a finger print of ordering of molecules during the deposition. The amount of order can be controlled by a chemical modification of molecules, as it was shown in the case of rotaxanes[18]. Thin films of catenane and fumaramide [2]rotaxane exhibit second harmonic generation activity[17,18]. In particular we have shown that in past that the films of rotaxane can be poled with electric field[18] as it is the case of functionalized polymers with active NLO chromophores. The films of the same fumaramide [2]rotaxane, deposited on a silver layer show an important structural order, which was tested by second harmonic generation measurements. The highest order is observed for macrocycle monolayers and the lowest for fumaramide [2]rotaxane multilayers, as expected. Theoretical calculations show that there is a large electric field above the silver layer which is at origin of the large SHG observed in these films. This field is a short range and disappears at a distance of about 9Å from silver surface. We obtain surprisingly good agreement between the calculated and measured values of about 9Å.

## ACKNOWLEDGMENTS

This work was performed within the EU RT network EMMMA contract n°: HPRN-CT-2002-00168 and received additional support from the EU contract MECHMOL n°: IST-2001-35504, from the FOM(Netherlands) and the Breedtestrategie program of the Rijksuniversiteit Groningen (NL).

## REFERENCES

1. A. G. Johnston, D. A. Leigh, R. J. Pritchard, M. D. Deegan, "Facile Synthesis and Solid-State Structure of a Benzylic Amide [2]Catenane**",** *Angew. Chem. Int. Ed. Engl*. 34, 1209-1212 (1995).
2. A.G. Johnston, D.A. Leigh, A. Murphy, J.P. Smart and M.D. Deegan, "The Synthesis and Solubilization of Amide Macrocycles via Rotaxane Formation", *J. Am. Chem. Soc.* 118, 10662-10663 **(**1996).
3. A G Johnston, D A Leigh, L Nezhat, J P Smart and M D Deegan, "Structurally Diverse and Dynamically Versatile Benzylic Amide [2]Catenanes Assembled Directly from Commercially Available Precursors", *Angew Chem. Int. Ed. Engl*. 34, 1212-1216 (1995).
4. F G Gatti, D A Leigh, S A Nepogodiev, A M Z Slawin, S J Teat and J K Y Wong, "Stiff, and Sticky in the Right Places: The Dramatic Influence of Preorganizing Guest Binding Sites on the Hydrogen Bond-Directed Assembly of Rotaxanes", *J. Am. Chem. Soc.* 123, 5983-5989 (2001).
5. Lane, A. S.; Leigh, D. A.; Murphy, A. "Peptide-Based Molecular Shuttles", *J. Am. Chem. Soc.* 119, 11092 (1997).
6. M. Whelan, F. Cecchet, R. Baxter, F. Zerbetto, G. J. Clarkson, D. A. Leigh and P. Rudolf, "Adsorption of a Benzylic Amide Macrocycle on a Solid Substrate: XPS and HREELS Characterization of Thin Films Grown on Au(111)", *J. Phys. Chem. B* 106, 8739-8746 (2002).
7. C.-A. Fustin, R. Gouttebaron, C. De Nadaï, R. Caudano, P. Rudolf, F. Zerbetto and D. A. Leigh, "Photoemission study of pristine and potassium intercalated benzylic amide [2]catenane films", *Surface Science* 474, 37-46 (2001).
8. C. A. Fustin, P. Rudolf, A. F. Taminiaux, F. Zerbetto, D. A. Leigh and R. Caudano, "Growth and Characterisation of Benzylic Amide [2]Catenane Thin Films", *Thin Solid Film*s 327-329, 321-325 (1998).
9. J. W. Ponder, F. J. Richards, "An Efficient Newton-Like Method for Molecular Mechanics Energy Minimization of Large Molecules", *J. Comput. Chem.*, 8, 1016-1026 (1987).

10. A. K. Rappe, W. A. Goddard III, “Charge Equilibration for Molecular-Dynamics Simulations”, *J. Phys. Chem.*, 95, 3358-3363 (1991).
11. C. Kundrot, J. W. Ponder , F. J. Richards,“ Algorithms for Calculating Excluded Volume and its Derivatives as a Function of Molecular Conformation and Their Use in Energy Minimization”, *J. Comput. Chem.*, 12, 402-409 (1991**).**
12. M. J. Dudek, J. W. Ponder, “Accurate Modeling of the Intramolecular Electrostatic Energy of Proteins”, J. *Comput. Chem.*, 16, 791-816 (1995).
13. W. Rocchia, E. Alexov, B. Honig, ” Extending the Applicability of the Nonlinear Poisson-Boltzmann Equation: Multiple Dielectric Constants and Multivalent Ions”, *J. Phys. Chem. B*, 105, 6507-6514 (2001).
14 N. L. Allinger, Y. H. Yuh, J.-H. Lii,“ Molecular mechanics. The MM3 force field for hydrocarbons. 1“, *J. Am. Chem. Soc.*, 111, 8551-8566 (1989).
15. T. Gase, D. Grando, P.-A. Chollet, F. Kajzar, A., Murphy and D. A. Leigh, “Linear and Unanticipated Second-Order Nonlinear Optical Properties of Benzylic Amide [2]Catenane Thin Films: Evidence of Partial Rotation of the Interlocked Molecular Rings in the Solid State” , *Adv. Mater*., 11, No. 15, 1303-1306, (1999)
16. M Choy and R. L. Byer, *Phys. Rev*. B14, 16993,(1976)
17. T. Gase, D. Grando, P.-A. Chollet, F. Kajzar, A. Lorin, D. A. Leigh and D. Tetard, “Thin Films of a Benzylic Amide [2]Catenane as a Novel Versatile Photonic Material”, *Nonlinear Opt*., 22, 491-6(1999)
18. V. Bermudez, T. Gase, F. Kajzar, N. Capron, F. Zerbetto, F. G. Gatti, D. A. Leigh and S. Zhang, “Rotaxanes – Novel Photonic Molecules”, *Opt.Mat*., 21, 39-44(2002)